33RD INTERNATIONAL COSMIC RAY CONFERENCE, RIO DE JANEIRO 2013
THE ASTROPARTICLE PHYSICS CONFERENCE

ICRC 2013

Kinetic Studies of Nonrelativistic Young Supernova Remnant Shocks

JACEK NIEMIEC[1], MARTIN POHL[2,3], ANTOINE BRET[4], VOLKMAR WIELAND[2,3].

[1] *Institute of Nuclear Physics, Polish Academy of Sciences, Radzikowskiego 152, 31-342 Kraków, Poland*
[2] *DESY, Platanenallee 6, 15738 Zeuthen, Germany*
[3] *Institute of Physics and Astronomy, University of Potsdam, 14476 Potsdam, Germany*
[4] *ETSI Industriales, Universidad de Castilla-La Mancha, 13071 Ciudad Real, Spain*

jacek.niemiec@ifj.edu.pl

Abstract: The structure of SNR shocks and the injection of suprathermal particles into a Fermi-type acceleration at such shocks constitute important problems of high-energy astrophysics. We report on recent results of kinetic particle-in-cell studies of nonrelativistic plasma collisions with absent or parallel large-scale magnetic field, that use parameter values expected for young SNRs. We show that the electron dynamics play an important role in the development of the system. While nonrelativistic shocks in both unmagnetized and magnetized plasmas can be mediated by Weibel-type instabilities, the efficiency of shock formation processes is higher when a large-scale magnetic field is present. The electron distributions downstream of the forward and reverse shocks are generally isotropic, whereas that is not always the case for the ions. We do not see any significant evidence of pre-acceleration, neither in the electron population nor in the ion distribution. First results of plasma collisions with perpendicular magnetic field configurations will also be presented. These simulations are based on a new setup that is unusually clean and permits the magnetic field strength and configuration to be different in the two colliding plasma slabs. We will also report on new realistic studies of the non-linear evolution and saturation of cosmic-ray streaming instabilities leading to the magnetic-field amplification upstream of the shock.

Keywords: acceleration of particles, instabilities, numerical methods, shock waves, supernova remnants

1 Introduction

Shell-type supernova remnants (SNR) are ideal laboratories for the study of particle acceleration at nonrelativistic collisionless shocks. The unsolved problem of injection is the most critical ingredient in the theory of particle acceleration at shocks, because it determines the level of cosmic-ray feedback and hence the nonlinearity of the system. Understanding of the latter is required for an appropriate treatment of cosmic-ray acceleration on larger scales, on which the quasi-thermal plasma may be described as a fluid and on which observational data can be obtained with existing γ-ray observatories and future installations such as Cherenkov Telescope Array (CTA).

In this work we report on our studies of the microphysics of nonrelativistic shocks with the method of kinetic particle-in-cell (PIC) simulations. Such simulations are the appropriate tool to study particle injection into shock acceleration because this process is a kinetic problem that cannot be addressed with MHD or other fluid techniques. This also includes hybrid simulations that assume a massless electron fluid, thus neglecting electron-scale effects that lead to scattering and heating. The results of our recent studies of *parallel* nonrelativistic shocks are summarized in section 2. In section 3 a newly developed setup for *perpendicular* shock simulation studies is presented. First results of plasma collisions with perpendicular magnetic field configurations and the results of realistic studies of the non-linear evolution and saturation of magnetic-field amplification processes induced by cosmic-ray streaming instabilities in the shock precursor will be reported at the conference.

2 Nonrelativistic Parallel Shocks

Contrary to earlier expectations that low-frequency electromagnetic ion-beam instabilities are the sources of the necessary dissipation at nonrelativistic shocks, recent simulations by [1] suggested that Weibel-type instabilities instead can trigger shock formation in an unmagnetized environment even for collisions with non-relativistic velocity. A pre-existing magnetic field may therefore be not necessary for the formation of non-relativistic shocks. We have performed 2D3V PIC simulations of non-relativistic plasma collisions with absent or parallel large-scale magnetic field. The question we addressed in this study is whether or not the shock structure and the particle spectra reach a steady state, and to what degree a parallel magnetic field renders shock formation more efficient. A secondary goal was to investigate the efficacy of particle preacceleration, which appears needed for their injection into a diffusive shock-acceleration process.

To address these questions we follow the evolution of the system longer than was done in [1]. Also, we are interested in asymmetric flows, i.e., the collision of plasma slabs of different density, leading to two different shocks and a contact discontinuity (CD) which is self-consistently modeled. The presentation in this section is based on our results recently published in [2].

Figures 1 and 2 present the final structure of the colliding plasma of our two main numerical experiments for unmagnetized plasma conditions (run U1) and for a weakly magnetized plasma (run M1), in which the plasma flow is aligned with the homogeneous magnetic field. Both simulations assume two electron-ion plasma streams of different densities to collide with each other at relative speed $v_{\rm rel} = 0.38c$. The density ratio between the *dense* (left,

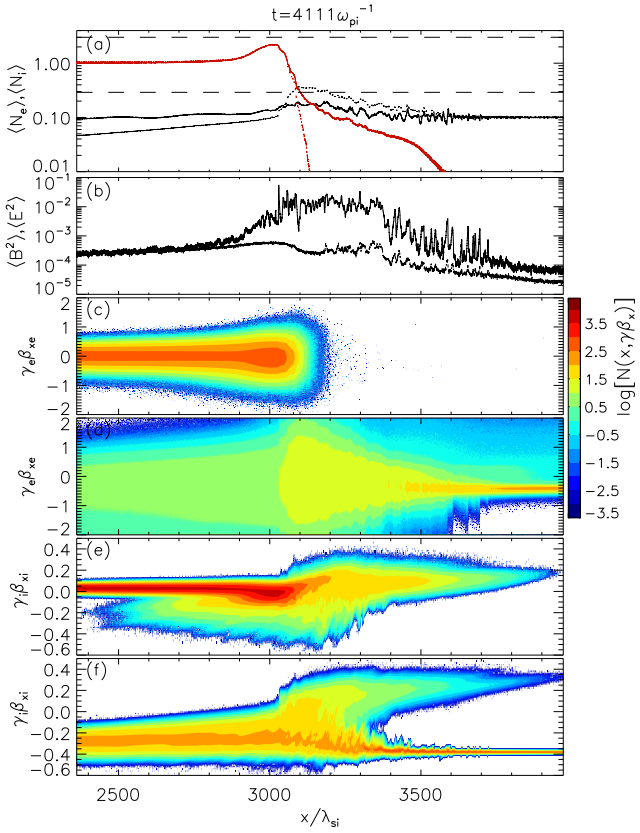

Figure 1: Structure of the collision region at the end of the simulation U1 with unmagnetized plasma at time $t = 4111\,\omega_{pi}^{-1}$. Shown are the profiles of (a) the average particle-number density normalized to the far-upstream density of the dense plasma (red lines: dense plasma, black lines: tenuous plasma; solid lines: ions, dotted lines: electrons), and (b) the average magnetic (solid line) and electric (dotted line) energy density in simulation units, and the longitudinal phase-space distributions separately for all particle species: electrons of the dense (c) and tenuous (d) plasma and ions of the dense (e) and tenuous (f) component. In panel (a), the horizontal dashed lines mark the hydrodynamic compression level of 2.9 for the forward shock (lower line) and 3.01 for the reverse shock (upper line).

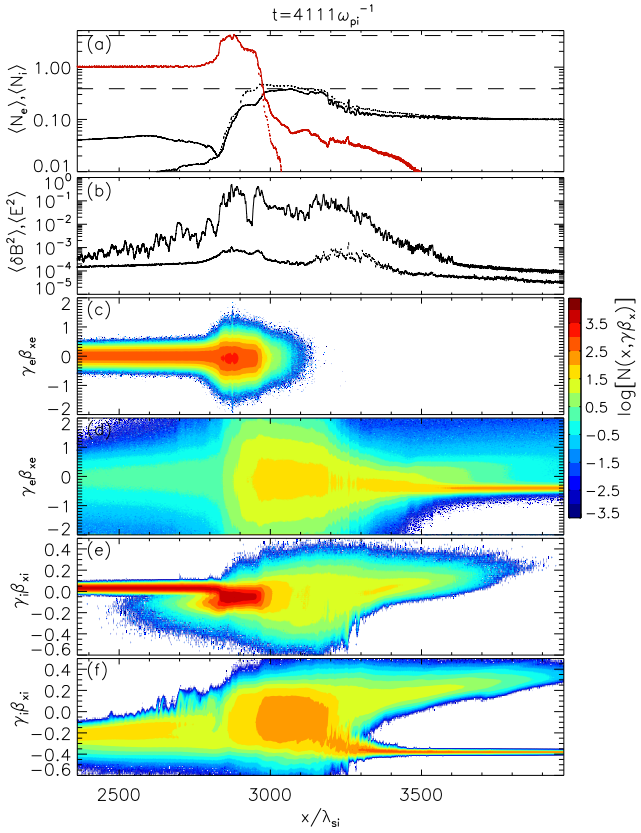

Figure 2: Structure of the collision region at the end of the magnetized simulation M1 at time $t = 4111\,\omega_{pi}^{-1}$ (see figure 1). The mean magnetic field contribution is subtracted in the magnetic energy-density profile in panel (b).

moving to the right in $+x$-direction) and the *tenuous* (right, moving to the left) plasma slab is 10 and the simulation is conducted in the center-of-momentum frame of the two plasmas. Both runs use an ion-electron mass ratio $m_i/m_e = 50$. The simulation setup is designed to be applicable to young SNRs, in which dense supernova ejecta propagating with nonrelativistic velocity collide with a dilute weakly-magnetized interstellar medium.

Both in the unmagnetized and the magnetized case, a double-shock structure builds on time scales of about a thousand ion plasma times, ω_{pi}^{-1}. The formation of these shocks is mediated by Weibel-type instabilities that are known from relativistic shocks. These instabilities lead to current filamentation and the generation of transverse magnetic fields. We show that while non-relativistic shocks in both unmagnetized and magnetized plasmas can be mediated by Weibel-type instabilities, the efficiency of shock-formation processes is higher when a large-scale parallel magnetic field is present. This can be seen through comparison of the average particle density profiles and phase-space distributions in Figures 1 and 2. It is evident from panel 1f that in the unmagnetized conditions the dilute-ion beam is not decoupled from the dense plasma and, despite being hot, continues to carry a substantial bulk-flow energy across the CD. Consequently, the forward-shock[1] compression ratio carries a substantial contribution from the dense ions, which play a role of the shock-reflected particles, needed to maintain the shock. On the other hand, in the magnetized case, the ion compression at the forward shock is almost entirely provided by the tenuous plasma, cf. panel 2a. Although the contribution of the dense ions to the number density of particles returning upstream is comparable to that of the tenuous ions (panels 2e-f), the latter represent a more directed and faster flow deep in the forward-shock precursor and also completely dominate the precursor dynamics further upstream. Thus, the forward shock begins to resemble a self-propagating structure that is exclusively maintained by shock-reflected particles, independent of the processes operating at and behind the CD. This is not yet the case in the dense plasma region. However, the compression ratio at the reverse shock reaches ~ 4, in agreement with the hydrodynamical jump conditions, and the dynamics of the deep reverse-shock precur-

1. Here, as forward shock we denote the shock propagating into the low-density (right, ambient) plasma; vice versa the reverse shock travels through the dense (left) plasma, that represents the ejecta.

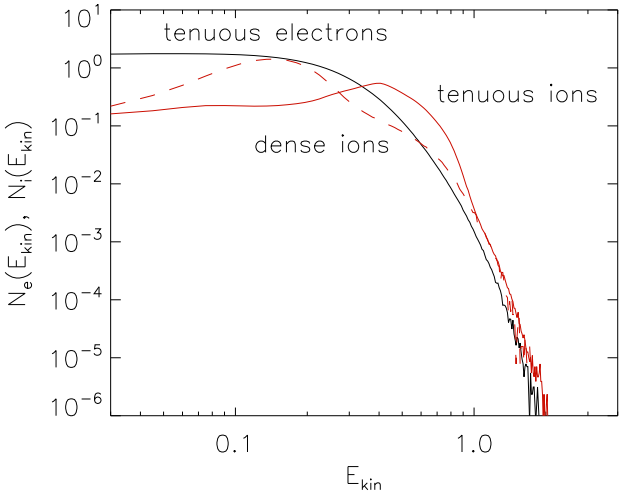

Figure 3: Kinetic-energy spectra of particles downstream of the forward shock at $x/\lambda_{si} \approx 3120$ (Figure 1) and time $t = 4111\,\omega_{pi}^{-1}$ for the unmagnetized run U1, in the CD rest frame. In simulation units $E_{\rm kin} = 0.25\,(\gamma-1)$ for electrons and $E_{\rm kin} = 12.5\,(\gamma-1)$ for ions. Normalized spectra are shown for tenuous electrons (black solid line), tenuous ions (red solid line), and the dense ions (red dashed line).

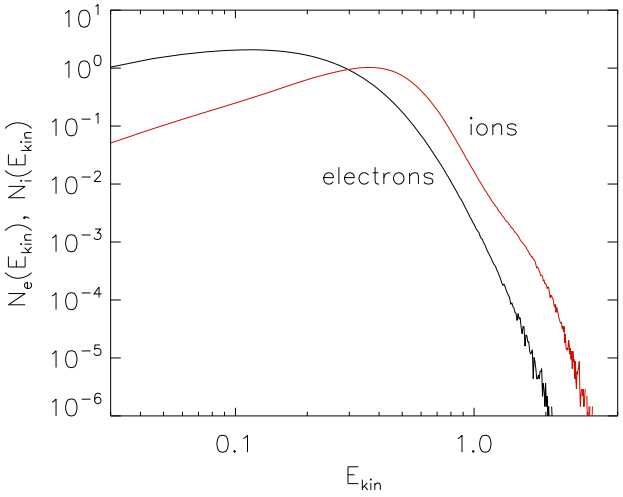

Figure 4: Kinetic-energy spectra of tenuous electrons (black line) and tenuous ions (red line) in the forward-shock downstream region at $x/\lambda_{si} \approx 3000$ (Figure 2) and time $t = 4111\,\omega_{pi}^{-1}$ for the magnetized run M1.

sor ($2750 \leq x/\lambda_{si} \leq 2820$) is solely governed by the shock-reflected dense ions. As can be observed in Figure 1, the reverse-shock transition in the unmagnetized simulation has not yet reached the compression ratio of a hydrodynamic shock.

The amplitude of magnetic turbulence generated in the collision region is in the magnetized plasma an order of magnitude larger than in unmagnetized conditions. The typical magnetization of the ambient medium, into which young SNR shocks propagate, given by $\sigma = M_{\rm A}^{-2}$, is in the range $10^{-6} < \sigma < 10^{-3}$. Our magnetized run with $\sigma \approx 2 \times 10^{-3}$ thus probes an upper limit of the sigma parameter, and any realistic formation scenario of parallel shocks in SNRs should show characteristics intermediate between the two cases studied here.

In the unmagnetized case, small-scale electrostatic and filamentation-like instabilities operate in parallel and heat the electrons. Eventually, strong fluctuations arise in the density of electrons and ions that lead to the formation of the double-shock structure. Thus, electron dynamics play an important role in the development of the system. Ion-ion or ion-electron streaming generally drives the turbulence, which is mainly magnetic. The exact type of an instability, however, depends on the location in the shock precursor and is generally different for forward and reverse shocks. In the magnetized case, filamentation in the dense plasma region is initially more pronounced. It provides a mechanism to efficiently decouple the colliding ion beams. Later this instability evolves into an oblique mode and nonlinear density fluctuations. Some of the streaming instabilities that lead to the formation of the reverse shock compression during late-stage evolution are similar to non-resonant modes that have been discussed in the context of cosmic-ray induced magnetic-field amplification, e.g., [3, 4, 5, 6, 7, 8]. In both the magnetized and unmagnetized systems, magnetic-field generation processes lead to stronger magnetic fields downstream of the forward shocks, rather than reverse shocks. We would thus expect synchrotron emission to originate from the magnetized structure of the forward shock transition, which is in agreement with SNR observations.

We have also studied the effect of the assumed ion-to-electron mass ratio on our results. We find that although the main characteristics of the long-time evolution of the systems do not critically depend on the mass ratio within the range studied, the detailed mechanisms of reaching a steady state might be modified or even different if the assumed mass ratio is too low. The timescales for particle-energy equilibration and the efficiency of particle pre-acceleration processes might be overestimated in simulations that use a reduced ion-to-electron mass ratio.

Particle spectra in kinetic energy, $E_{\rm kin} = (\gamma - 1) m_l c^2\,(m_l = m_e, m_i)$, downstream of the forward shock in the CD rest frame are presented in Figures 3 and 4, for the

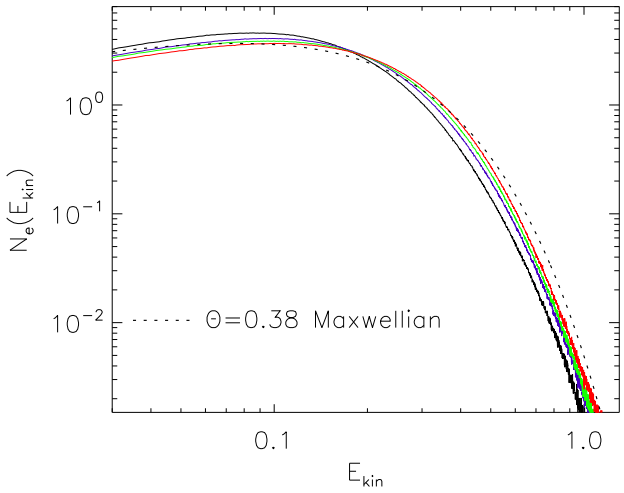

Figure 5: Tenuous-electron kinetic-energy spectra in the forward-shock downstream region at $\sim 50\lambda_{si}$ from the CD at times $t = 2406$ (black line), 2974 (blue line), 3542 (green line), and $4111\,\omega_{pi}^{-1}$ (red line) for run M1. The dotted line shows a relativistic Maxwellian for comparison.

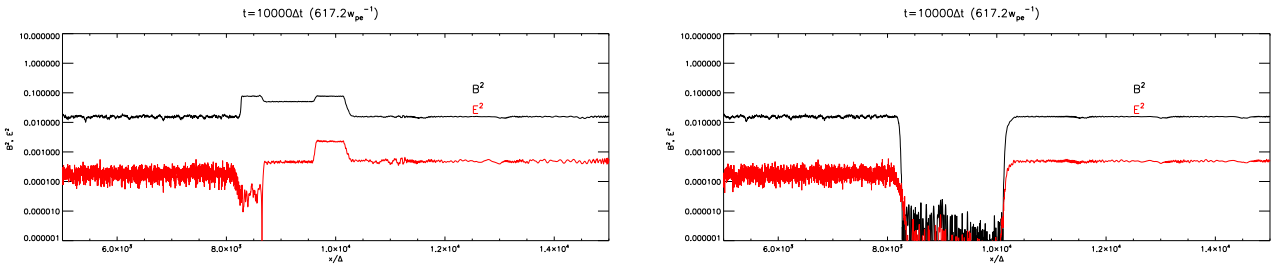

Figure 6: Stability comparison of a setup with constant perpendicular magnetic field B_z, which has a jumping motional electric field E_y (*left panel*), and the new setup with a transition zone (*right panel*), both after 10000 time steps. The middle of the simulation box is at $x = 10000$ and the edges of the two plasmas started - in this demonstration simulation - at $x = 8000$ and $x = 12000$. The void between the two plasmas, still about 1500 gridcells wide in this test simulation, is largely free of electromagnetic fields with our new setup, but full of strong transient fields if the standard method is used.

unmagnetized and magnetized case, respectively. The electron distributions are generally isotropic and quasi-thermal. The electrons carry nearly as much kinetic energy as do the ions. The latter have not yet reached an equilibrium and their distributions are very anisotropic. In the unmagnetized case, Figure 3, both the dense and tenuous ions contribute to the ion energy spectrum and the spectral components formed by the decelerated tenuous and dense ion beams can be identified. In both the magnetized and unmagnetized case, the high-energy tails are built by heated beam particles and ions returning upstream. These superficial tails are thus not indicative of ion pre-acceleration.

Likewise, we do not see any significant evidence of pre-acceleration in the electron population. The time evolution of the electron spectra in run M1, Figure 5, displays a slow increase in average energy. However, after renormalization of the spectra to dimensionless energy $x = E/E_{\rm kin,av}$, with the average particle energy $E_{\rm kin,av}$, the shape of the spectra evolves very weakly. It is thus mainly a continuous increase in $E_{\rm kin,av}$ that is responsible for the spectral evolution, not the development of a supra-thermal tail.

3 Nonrelativistic Perpendicular Shocks

Published simulations of non-relativistic perpendicular shocks indicate a rapid shock formation and efficient pre-acceleration of particles [9, 10, 11]. However, the simulation setup typically involves large localized gradients in either the electric or the magnetic field, that act as an artificial antenna during the start-up phase of the simulation. To circumvent this problem we have developed a new setup that permits relatively clean simulations with perpendicular magnetic fields.

With all methods of shock generation, any perpendicular magnetic field must be embedded in moving plasma, thus requiring a motional electric field on account of the Lorentz transformation of the magnetic field. In the collision zone (or at the reflecting wall, if that is used) a strong gradient in the motional electric field will be imposed which acts as an antenna through large $\vec{\nabla} \times \vec{E}$ contributions, thus inducing a transient that may limit the veracity of the simulation. We avoid most of that transient by letting the perpendicular field fall off at the front of each plasma slab and imposing a current sheet in front of each plasma slab that compensates $\vec{\nabla} \times \vec{B}$, thus maintaining $\partial \vec{E}/\partial t = 0$, while permitting the perpendicular field to quickly fall off with distance from the plasma slab. If the current is carried by particles that drift slowly enough to avoid Buneman-type instabilities, each plasma slab is stable in the simulation for a time period given by the Larmor timescale, and instabilities only arise from the collision.

Figure 6 compares the stability of a setup with a constant perpendicular out-of-plane magnetic field B_z throughout the simulation box, which has a jumping motional electric field E_y, and the new setup with the transition zone described above. One can clearly see, that the new setup is very stable over many time steps, whereas the standard setup is not stable. In fact, in the standard scenario a transient in the electric field is emitted at the strong field gradient in the center of the simulation box, where the approaching plasma slabs have not yet arrived. Thus, the plasma would be artificially accelerated before the slabs collide.

Besides providing a clean initial conditions, our new setup permits the modeling of two shocks in parallel, because each of the colliding plasmas develops a shock. We can also account for different densities and different magnetizations of the plasma slabs, something that is impossible with the reflecting-wall method.

First results of plasma collisions with perpendicular magnetic field configurations will be presented at the conference.

Acknowledgment: The work of J.N. is supported by NCN through research projects DEC-2011/01/B/ST9/03183 and DEC-2011/01/M/ST9/01891. M.P. and V.W. acknowledge support through grant PO 1508/1-1 of the Deutsche Forschungsgemeinschaft. The work of A.B. is supported by the project ENE2009-09276 of the Spanish Ministerio de Educacion y Ciencia. Simulations have been performed at the Pleiades facility at the NASA Advanced Supercomputing (NAS).

References

[1] Kato, T. N., & Takabe, H., 2008, ApJ, 681, L93
[2] Niemiec, J., Pohl, M., Bret, A., & Wieland, V., 2012, ApJ, 759, 73
[3] Bell, A.R., 2007, MNRAS, 353, 550
[4] Niemiec, J., Pohl, M., Stroman, T., & Nishikawa, K.-I., 2008, ApJ, 684, 1174
[5] Riquelme, M. A., & Spitkovsky, A., 2009, ApJ, 694, 626
[6] Stroman, T., Pohl, M., & Niemiec, J., 2009, ApJ, 706, 38
[7] Niemiec, J., Pohl, M., Bret, A., & Stroman, T., 2010, ApJ, 709, 1148
[8] Stroman, T., Pohl, M., Niemiec, J., Bret, A., 2012, ApJ, 746, 24
[9] Murphy, G. C., Dieckmann, M. E., Bret, A., & Drury, L. O., 2010, A&A, 524, A84
[10] Riquelme, M. A., & Spitkovsky, A., 2011, ApJ, 733, 63
[11] Gargate, L., & Spitkovsky, A., 2012, ApJ, 744, 67